

A Unified Performance Analysis of Free-Space Optical Links Over Gamma-Gamma Turbulence Channels with Pointing Errors

Imran Shafique Ansari*, Ferkan Yilmaz**, and Mohamed-Slim Alouini*

*Computer, Electrical, and Mathematical Sciences and Engineering (CEMSE) Division,
King Abdullah University of Science and Technology (KAUST),
Thuwal, Makkah Province, Kingdom of Saudi Arabia

**Vodafone Technology in Turkey, ITU ARI-3 Teknokent, 34467,
Koruyolu, Maslak, Sariyer, Istanbul, Turkey

Email: {imran.ansari, slim.alouini}@kaust.edu.sa, ferkan.yilmaz@vodafone.com

Abstract—In this work, we present a unified performance analysis of a free-space optical (FSO) link that accounts for pointing errors and both types of detection techniques (i.e. intensity modulation/direct detection as well as heterodyne detection). More specifically, we present unified exact closed-form expressions for the cumulative distribution function, the probability density function, the moment generating function, and the moments of the end-to-end signal-to-noise ratio (SNR) of a single link FSO transmission system, all in terms of the Meijer’s G function except for the moments that is in terms of simple elementary functions. We then capitalize on these unified results to offer unified exact closed-form expressions for various performance metrics of FSO link transmission systems, such as, the outage probability, the higher-order amount of fading (AF), the average error rate for binary and M -ary modulation schemes, and the ergodic capacity, all in terms of Meijer’s G functions except for the higher-order AF that is in terms of simple elementary functions. Additionally, we derive the asymptotic results for all the expressions derived earlier in terms of Meijer’s G function in the high SNR regime in terms of simple elementary functions via an asymptotic expansion of the Meijer’s G function. We also derive new asymptotic expressions for the ergodic capacity in the low as well as high SNR regimes in terms of simple elementary functions via utilizing moments. All the presented results are verified via computer-based Monte-Carlo simulations.

Index Terms—Free-space optical (FSO) communications, optical wireless communications, pointing errors, Gamma-Gamma turbulence channels, outage probability (OP), binary modulation schemes, bit-error rate (BER), symbol error rate (SER), amount of fading (AF), ergodic capacity, Meijer’s G function.

I. INTRODUCTION

IN recent times, radio frequency (RF) spectrum scarcity has become the biggest and prime concern in the arena of wireless communications. Due to this RF spectrum scarcity, additional RF bandwidth allocation, as utilized in the recent past, is not anymore a viable solution to fulfill the demand for higher data rates [1]. Of the many other popular solutions, free-space optical (FSO) or optical wireless communication systems have gained an increasing interest due to its advantages

including higher bandwidth and higher capacity compared to the traditional RF communication systems. In addition, FSO links are license-free and hence are cost-effective relative to the traditional RF links. It is a promising technology as it offers full-duplex Gigabit Ethernet throughput in certain applications and environment offering a huge license-free spectrum, immunity to interference, and high security [2]. These features of FSO communication systems potentially enable solving the issues that the RF communication systems face due to the expensive and scarce spectrum [2]–[8]. Besides these nice characteristic features of FSO communication systems, they span over long distances of 1Km or longer. However, the atmospheric turbulence may lead to a significant degradation in the performance of the FSO communication systems [3].

Additionally, thermal expansion, dynamic wind loads, and weak earthquakes result in the building sway phenomenon that causes vibration of the transmitter beam leading to a misalignment between transmitter and receiver known as pointing error. These pointing errors may lead to significant performance degradation and are a serious issue in urban areas, where the FSO equipments are placed on high-rise buildings [9]–[11].

It is worthy to learn that intensity modulation/direct detection (IM/DD) is the main mode of detection in FSO systems but coherent communications have also been proposed as an alternative detection mode. Among these, heterodyne detection is a more complicated detection method but has the ability to better overcome the thermal noise effects (see [9], [10], [12], [13] and references cited therein).

Over the last couple of decades, ample amount of work has been done on studying the performance of a single FSO link operating over Gamma-Gamma fading channels with and without pointing errors in the presence of IM/DD or heterodyne detection techniques (see [10]–[19] and references cited therein). However as per authors best knowledge, there are no unified expressions nor asymptotic expressions that capture the performance of both these systems. Hence, in this work we present a unified approach for the calculation of the probability density function (PDF), the cumulative distribution function (CDF), and the moment generating function (MGF)

of a single FSO link in exact closed-form in terms of Meijer's G function, and the moments in terms of simple elementary functions. Besides, we also present the outage probability (OP), the bit-error rate (BER) of binary modulation schemes, the symbol error rate (SER) of M -ary amplitude modulation (M-AM), M -ary phase shift keying (M-PSK) and M -ary quadrature amplitude modulation (M-QAM), and the ergodic capacity also in terms of Meijer's G functions, and the higher-order amount of fading (AF) in terms of simple elementary functions. Further, we derive the asymptotic expressions for all the expressions derived earlier in terms of Meijer's G function at high signal-to-noise ratio (SNR) regime in terms of simple elementary functions via Meijer's G function expansion, and additionally, we derive the ergodic capacity at low and high SNR regimes in terms of simple elementary functions via utilizing moments.

The remainder of the paper is organized as follows. Section II presents a single unified FSO link system and channel model accounting for pointing errors with both type of detection technique (IM/DD and heterodyne) followed by Section III that presents exact closed form expressions and the asymptotic expressions for the statistical characteristics of a single unified FSO link including the CDF, the PDF, and the MGF in terms of Meijer's G functions and simple elementary functions respectively. Subsequently, the performance metrics under consideration, namely, the OP, the higher-order AF, the BER, the SER, and the ergodic capacity are presented in terms of unified expressions and asymptotic expressions in Section IV. Finally, Section V presents some simulation results to validate these analytical results followed by concluding remarks in Section VI.

II. CHANNEL AND SYSTEM MODELS

We assume that we employ an FSO link that experiences Gamma-Gamma fading with pointing error impairments for which the PDF of the receiver irradiance I is given by [11, Eq. (8)] or in a more simpler form utilizing [20, Eq. (6.2.4)] as

$$f_I(I) = \frac{\xi^2}{I\Gamma(\alpha)\Gamma(\beta)} G_{1,3}^{3,0} \left[\alpha \beta \frac{I}{A_0} \left| \begin{matrix} \xi^2 + 1 \\ \xi^2, \alpha, \beta \end{matrix} \right. \right], \quad (1)$$

where ξ is the ratio between the equivalent beam radius at the receiver and the pointing error displacement standard deviation (jitter) at the receiver [10], [11] (i.e. when $\xi \rightarrow \infty$, (1) converges to the non-pointing errors case), A_0 is a constant term that defines the pointing loss, α and β are the fading/scintillation parameters¹ related to the atmospheric turbulence conditions [2], [4], [5] with lower values of α and β indicating severe atmospheric turbulence conditions, $\Gamma(\cdot)$ is the Gamma function as defined in [24, Eq. (8.310)], and $G[\cdot]$ is the Meijer's G function as defined in [24, Eq. (9.301)].

¹Note that the parameters α and β vary depending on the type (plane or spherical) of wave propagation [21] being assumed. Hence, α and β are not chosen arbitrarily instead they can be determined from the Rytov variance [22]. In case of plane wave propagation, α and β may be determined via [10, Eq. (3)] whereas in case of spherical wave propagation, α and β may be determined utilizing [11, Eqs. (4) and (5)]. Also, the relation $\alpha > \beta$ always holds [23].

For the heterodyne detection technique case, the average SNR develops as $\mu_{\text{heterodyne}} = \eta_e \mathbb{E}_I[I]/N_0 = A_0 \eta_e \xi^2 / [(1 + \xi^2) N_0] \stackrel{\xi^2 \gg 1}{=} A_0 \eta_e / N_0$, where η_e is the effective photoelectric conversion ratio, N_0 symbolizes the additive white Gaussian noise (AWGN) sample, and $\mathbb{E}[\cdot]$ denotes the expectation operator. Alongside, with $\gamma = \eta_e I/N_0$, we get $I = A_0 \gamma / \mu_{\text{heterodyne}}$. On utilizing this simple random variable transformation, the resulting SNR PDF under the heterodyne detection technique is given as

$$f_{\gamma_{\text{heterodyne}}}(\gamma) = \frac{\xi^2}{\gamma \Gamma(\alpha)\Gamma(\beta)} G_{1,3}^{3,0} \left[\alpha \beta \frac{\gamma}{\mu_{\text{heterodyne}}} \left| \begin{matrix} \xi^2 + 1 \\ \xi^2, \alpha, \beta \end{matrix} \right. \right], \quad (2)$$

where $\mu_{\text{heterodyne}} = \mathbb{E}_{\gamma_{\text{heterodyne}}}[\gamma] = \bar{\gamma}_{\text{heterodyne}}$ is the average SNR² of (2). This PDF in (2) is in agreement with [10, Eq. (12)], [13, Eq. (4)].

Similarly, for the IM/DD detection technique case, the average electrical SNR develops as $\mu_{\text{IM/DD}} = \eta_e^2 \mathbb{E}_I^2[I]/N_0 = A_0^2 \eta_e^2 \xi^4 / [(1 + \xi^2)^2 N_0] \stackrel{\xi^2 \gg 1}{=} A_0^2 \eta_e^2 / N_0$ [11]. With $\gamma = \eta_e^2 I^2 / N_0$, we get $I = A_0 \sqrt{\gamma} / \mu_{\text{IM/DD}}$ [11]. On utilizing this simple random variable transformation, the resulting SNR PDF under the IM/DD technique is given as

$$f_{\gamma_{\text{IM/DD}}}(\gamma) = \frac{\xi^2}{2\gamma \Gamma(\alpha)\Gamma(\beta)} G_{1,3}^{3,0} \left[\alpha \beta \sqrt{\frac{\gamma}{\mu_{\text{IM/DD}}}} \left| \begin{matrix} \xi^2 + 1 \\ \xi^2, \alpha, \beta \end{matrix} \right. \right], \quad (3)$$

where $\mu_{\text{IM/DD}} = \mathbb{E}_{\gamma_{\text{IM/DD}}}[\gamma] \mathbb{E}_I^2[I] / \mathbb{E}_I[I]^2 \stackrel{\xi^2 \gg 1}{=} \bar{\gamma}_{\text{IM/DD}} \mathbb{E}_I^2[I] / \mathbb{E}_I[I]^2$ is the average SNR³ of (3), where $\mathbb{E}_I[I^2] / \mathbb{E}_I^2[I] - 1$ is defined as the scintillation index [22, Eq. (6)]. This PDF given in (3) is in agreement with [11, Eq. (20)].

Both these PDFs in (2) and (3) can be easily combined yielding the unified expression

$$f_{\gamma}(\gamma) = \frac{\xi^2}{r\gamma \Gamma(\alpha)\Gamma(\beta)} G_{1,3}^{3,0} \left[\alpha \beta \left(\frac{\gamma}{\mu_r} \right)^{\frac{1}{r}} \left| \begin{matrix} \xi^2 + 1 \\ \xi^2, \alpha, \beta \end{matrix} \right. \right], \quad (4)$$

where r is the parameter defining the type of detection technique (i.e. $r = 1$ represents heterodyne detection and $r = 2$ represents IM/DD). More specifically, for μ_r , when $r = 1$, $\mu_1 = \mu_{\text{heterodyne}}$ and when $r = 2$, $\mu_2 = \mu_{\text{IM/DD}}$. As a special case, for negligible pointing errors case under IM/DD technique (i.e. $\xi \rightarrow \infty$ and $r = 2$), (4) reduces to [11, Eq. (9)].

² $\bar{\gamma}_{\text{heterodyne}}$ is the average SNR for coherent/heterodyne FSO systems given by $\bar{\gamma}_{\text{heterodyne}} = C_c$ [22, Eq. (7)], where $C_c = 2 R^2 A P_{LO} / [2 q R \Delta f P_{LO} + 2 \Delta f (q R A I_b + 2 k_b T_k F_n / R_L)] \approx R A / (q \Delta f)$ is a multiplicative constant for a given heterodyne/coherent system, where R is the photodetector responsivity, A is the photodetector area, P_{LO} is the local oscillator power, Δf denotes the noise equivalent bandwidth of a FSO receiver, q is the electronic charge, I_b is the background light irradiance, k_b is Boltzmann's constant, T_k is the temperature in Kelvin, F_n represents a thermal noise enhancement factor due to amplifier noise, and R_L is the load resistance.

³ $\bar{\gamma}_{\text{IM/DD}}$ is the average SNR for IM/DD FSO systems given by $\bar{\gamma}_{\text{IM/DD}} = C_s (\alpha + 1) (\beta + 1) / (\alpha \beta)$ [22, Eq. (8)], where $C_s = (R A \xi^2) / [2 \Delta f (q R A I_b + 2 k_b T_k F_n / R_L)]$ is a multiplicative constant for a given IM/DD system.

It is important note here that one may easily derive a PDF corresponding to a certain detection technique from the PDF of the other corresponding detection technique via simple random variable transformation. For instance, (3) can be easily derived from (2) by transforming the random variable, γ , in (2) to $\gamma^2 \mu_{IM/DD}/\mu_{heterodyne}^2$ wherein this updated γ will represent the random variable of (3).

III. CLOSED-FORM STATISTICAL CHARACTERISTICS

A. Cumulative Distribution Function

Using [25, Eq. (07.34.21.0084.01)] and some simple algebraic manipulations, the CDF of γ can be shown to be given by

$$F_\gamma(\gamma) = \int_0^\gamma f_\gamma(t) dt = A G_{r+1, 3r+1}^{3r, 1} \left[\frac{B}{\mu_r} \gamma \middle| \begin{matrix} 1, \kappa_1 \\ \kappa_2, 0 \end{matrix} \right], \quad (5)$$

where $A = \frac{r^{\alpha+\beta-2} \xi^2}{(2\pi)^{r-1} \Gamma(\alpha) \Gamma(\beta)}$, $B = \frac{(\alpha\beta)^r}{r^{2r}}$, $\kappa_1 = \frac{\xi^2+1}{r}, \dots, \frac{\xi^2+r}{r}$ comprises of r terms, and $\kappa_2 = \frac{\xi^2}{r}, \dots, \frac{\xi^2+r-1}{r}, \frac{\alpha}{r}, \dots, \frac{\alpha+r-1}{r}, \frac{\beta}{r}, \dots, \frac{\beta+r-1}{r}$ comprises of $3r$ terms. This unified expression for the CDF of a single unified FSO link in (5) is in agreement with the individual results presented in [14, Eq. (15)] (for $\xi \rightarrow \infty$ and $r = 2$), [10, Eq. (15)] and [15, Eq. (17)] (for $r = 1$), [16, Eq. (16)] and [12, Eq. (7)] (for $\xi \rightarrow \infty$ and $r = 1$), and references cited therein.

Now, by using [20, Eq. (6.2.2)] to invert the argument in the Meijer's G function in (5) and then applying (26) from the Appendix, the CDF in (5) can be given asymptotically, at **high SNR**, in a simpler form in terms of basic elementary functions as

$$F_\gamma(\gamma) \underset{\mu_r \gg 1}{\approx} A \sum_{k=1}^{3r} \left(\frac{\mu_r}{B\gamma} \right)^{-\kappa_{2,k}} \frac{\prod_{l=1; l \neq k}^{3r} \Gamma(\kappa_{2,l} - \kappa_{2,k})}{\kappa_{2,k} \prod_{l=2}^{r+1} \Gamma(\kappa_{1,l} - \kappa_{2,k})}, \quad (6)$$

where $\kappa_{u,v}$ represents the v^{th} -term of κ_u . Subsequently, the asymptotic expression for the CDF in (6) is dominated by the $\min(\xi, \alpha, \beta)$ where ξ represents the 1st-term, α represents the $(r+1)^{\text{th}}$ -term, and β represents the $(2r+1)^{\text{th}}$ -term in κ_2 i.e. when the difference between the parameters is greater than 1 then the asymptotic expression for the CDF in (6) is dominated by a single term that has the least value among the above three parameters i.e. ξ, α , and β . On the other hand, if the difference between any two parameters is less than 1 then the asymptotic expression for the CDF in (6) is dominated by the summation of the two terms that have the least value among the above three parameters with a difference less than 1 and so on and so forth.

B. Moment Generating Function

The MGF defined as $\mathcal{M}_\gamma(s) \triangleq \mathbb{E}[e^{-\gamma s}]$, can be expressed, using integration by parts, in terms of CDF as

$$\mathcal{M}_\gamma(s) = s \int_0^\infty e^{-\gamma s} F_\gamma(\gamma) d\gamma. \quad (7)$$

By placing (5) into (7) and utilizing [24, Eq. (7.813.1)], we get after some manipulations the MGF of γ as

$$\mathcal{M}_\gamma(s) = A G_{r+2, 3r+1}^{3r, 2} \left[\frac{B}{\mu_r s} \middle| \begin{matrix} 0, 1, \kappa_1 \\ \kappa_2, 0 \end{matrix} \right]. \quad (8)$$

This unified expression for the MGF of a single unified FSO link in (8) is in agreement with the individual result presented in [26, Eq. (3)] (for $\xi \rightarrow \infty$ and $r = 2$), and references cited therein. Similar to the CDF, the MGF can be expressed asymptotically, at **high SNR**, as

$$\mathcal{M}_\gamma(s) \underset{\mu_r \gg 1}{\approx} A \sum_{k=1}^{3r} \left(\frac{s}{B} \mu_r \right)^{-\kappa_{2,k}} \times \frac{\prod_{l=1; l \neq k}^{3r} \Gamma(\kappa_{2,l} - \kappa_{2,k}) \prod_{l=1}^2 \Gamma(1 + \kappa_{2,k} - \kappa_{1,l})}{\Gamma(1 + \kappa_{2,k}) \prod_{l=3}^{r+2} \Gamma(\kappa_{1,l} - \kappa_{2,k})}, \quad (9)$$

and can be further expressed via only the dominant term(s) based on a similar explanation to the one given for the CDF case earlier.

C. Moments

The moments are defined as $\mathbb{E}[\gamma^n]$. Placing (5) into the definition and utilizing [24, Eq. (7.813.1)], we derive, to the best of our knowledge, a new expression for the moments in exact closed-form and in terms of simple elementary functions as

$$\mathbb{E}[\gamma^n] = \frac{\xi^2 \Gamma(rn + \alpha) \Gamma(rn + \beta)}{(\alpha\beta)^{rn} (rn + \xi^2) \Gamma(\alpha) \Gamma(\beta)} \mu_r^n. \quad (10)$$

It is worthy to note that this simple result for the moments is particularly useful to conduct asymptotic analysis of the ergodic capacity in the later part of this work.

IV. APPLICATIONS

A. Outage Probability

When the instantaneous output SNR γ falls below a given threshold γ_{th} , we encounter a situation labeled as outage and it is an important feature to study OP of a system. Hence, another important fact worth stating here is that the expressions derived in (5) and (6) also serve the purpose for the expressions of OP for a FSO channel or in other words, the probability that the SNR falls below a predetermined protection ratio γ_{th} can be simply expressed by replacing γ with γ_{th} in (5) and (6) as

$$P_{\text{out}}(\gamma_{\text{th}}) = F_\gamma(\gamma_{\text{th}}). \quad (11)$$

B. Higher-Order Amount of Fading

The AF is an important measure for the performance of a wireless communication system as it can be utilized to parameterize the distribution of the SNR of the received signal. In particular, the n^{th} -order AF for the instantaneous SNR γ is defined as [27]

$$AF_\gamma^{(n)} = \frac{\mathbb{E}[\gamma^n]}{\mathbb{E}[\gamma]^n} - 1. \quad (12)$$

Now, utilizing (12) by substituting (10) into it, we get the n^{th} -order AF as

$$AF_\gamma^{(n)} = \frac{(r + \xi^2)^n [\Gamma(\alpha) \Gamma(\beta)]^{n-1} \Gamma(rn + \alpha) \Gamma(rn + \beta)}{\xi^{n-1} (rn + \xi^2) [\Gamma(r + \alpha) \Gamma(r + \beta)]^n} - 1. \quad (13)$$

For $n = 2$, as a special case, we get the classical AF [28] as

$$AF = AF_\gamma^{(2)} = \frac{(r + \xi^2)^2 \Gamma(\alpha) \Gamma(\beta) \Gamma(2r + \alpha) \Gamma(2r + \beta)}{\xi (2r + \xi^2) [\Gamma(r + \alpha) \Gamma(r + \beta)]^2} - 1. \quad (14)$$

TABLE I
BER PARAMETERS OF BINARY MODULATIONS

Modulation	p	q
Coherent Binary Frequency Shift Keying (CBFSK)	0.5	0.5
Coherent Binary Phase Shift Keying (CBPSK)	0.5	1
Non-Coherent Binary Frequency Shift Keying (NBFSK)	1	0.5
Differential Binary Phase Shift Keying (DBPSK)	1	1

C. Average BER

Substituting (5) into [29, Eq. (12)] and utilizing [24, Eq. (7.813.1)], we get the average BER \bar{P}_b of a variety of binary modulations as

$$\bar{P}_b = \frac{A}{2\Gamma(p)} G_{r+2,3r+1}^{3r,2} \left[\frac{B}{\mu_r q} \middle| \begin{matrix} 1-p, 1, \kappa_1 \\ \kappa_2, 0 \end{matrix} \right], \quad (15)$$

where the parameters p and q account for different modulation schemes. For an extensive list of modulation schemes represented by these parameters, one may look into [29]–[32] or refer to Table I. This unified expression for the BER of a single unified FSO link in (15) is in agreement with the individual results presented in [33, Eq. (5)] (for $r = 2$), [10, Eq. (24)] (for $r = 1$), [12, Eq. (10)] and [34, Eq. (7)] (for $\xi \rightarrow \infty$ and $r = 1$), and references cited therein. Similar to the CDF, the BER can be expressed asymptotically, at **high SNR**, as

$$\begin{aligned} \bar{P}_b \underset{\mu_r \gg 1}{\approx} & \frac{A}{2\Gamma(p)} \sum_{k=1}^{3r} \left(\frac{q}{B} \mu_r \right)^{-\kappa_{2,k}} \\ & \times \frac{\prod_{l=1; l \neq k}^{3r} \Gamma(\kappa_{2,l} - \kappa_{2,k}) \prod_{l=1}^2 \Gamma(1 + \kappa_{2,k} - \kappa_{1,l})}{\Gamma(1 + \kappa_{2,k}) \prod_{l=3}^{r+2} \Gamma(\kappa_{1,l} - \kappa_{2,k})}, \end{aligned} \quad (16)$$

and can be further expressed via only the dominant term(s) based on a similar explanation to the one given for the CDF case earlier. Additionally, utilizing $\bar{P}_b \approx (G_c \mu_r)^{-G_d}$ [35, Eq. (1)], we can easily share that the diversity order $G_d = \min(\xi^2/r, \alpha/r, \beta/r) \underset{\alpha > \beta}{=} \min(\xi^2/r, \beta/r)$ and the coding gain is

$$\begin{aligned} G_c &= q/B (A / (2\Gamma(p))) \\ & \times \left(\frac{\prod_{l=1; l \neq k}^{3r} \Gamma(\kappa_{2,l} - \kappa_{2,k}) \prod_{l=1}^2 \Gamma(1 + \kappa_{2,k} - \kappa_{1,l})}{\Gamma(1 + \kappa_{2,k}) \prod_{l=3}^{r+2} \Gamma(\kappa_{1,l} - \kappa_{2,k})} \right)^{-\frac{1}{\kappa_{2,k}}}. \end{aligned} \quad (17)$$

D. Average SER

In [36], the conditional SER has been presented in a desirable form and utilized to obtain the average SER of M-AM, M-PSK, and M-QAM. For example, for M-PSK the average SER \bar{P}_s over generalized fading channels is given by [36, Eq. (41)]. Similarly, for M-AM and M-QAM, the average SER \bar{P}_s over generalized fading channels is given by [36, Eq. (45)] and [36, Eq. (48)] respectively. On substituting (8) into [36, Eq. (41)], [36, Eq. (45)], and [36, Eq. (48)], we can get the SER of M-PSK, M-AM, and M-QAM, respectively. The analytical SER performance expressions obtained via the above substitutions are exact and can be easily estimated accurately by utilizing

the Gauss-Chebyshev Quadrature (GCQ) formula [37, Eq. (25.4.39)] that converges rapidly, requiring only few terms for an accurate result [38].

E. Ergodic Capacity

The ergodic channel capacity \bar{C} is defined as $\bar{C} \triangleq \mathbb{E}[\log_2(1 + \gamma)]$. Utilizing this equation by placing (4) in it, using [25, Eq. (07.34.03.0456.01)] to represent $\ln(1 + \gamma)$ in terms of Meijer's G function as $G_{2,2}^{1,2} \left[\gamma \middle| \begin{matrix} 1, 1 \\ 1, 0 \end{matrix} \right]$, and using [39, Eq. (21)], the ergodic capacity can be expressed as

$$\bar{C} = \frac{A}{\ln(2)} G_{r+2,3r+2}^{3r+2,1} \left[\frac{B}{\mu_r} \middle| \begin{matrix} 0, 1, \kappa_1 \\ \kappa_2, 0, 0 \end{matrix} \right]. \quad (18)$$

This unified expression for the ergodic capacity of a single unified FSO link in (18) is in agreement with the individual results presented in [11, Eq. (22)] (for $r = 2$), [14, Eq. (21)] and [11, Eq. (11)] (for $\xi \rightarrow \infty$ and $r = 2$), [40, Eq. (10)] (for $r = 1$), [18, Eq. (16)] and [17, Eq. (3)] (for $\xi \rightarrow \infty$ and $r = 1$), and references cited therein. Similar to the CDF, the ergodic capacity can be expressed asymptotically via utilizing the Meijer's G function expansion given in the Appendix, at **high SNR**, as

$$\begin{aligned} \bar{C} \underset{\mu_r \gg 1}{\approx} & \frac{A}{\ln(2)} \sum_{k=1}^{3r+2} \left(\frac{\mu_r}{B} \right)^{-\kappa_{2,k}} \\ & \times \frac{\Gamma(1 + \kappa_{2,k}) \prod_{l=1; l \neq k}^{3r+2} \Gamma(\kappa_{2,l} - \kappa_{2,k})}{\prod_{l=2}^{r+2} \Gamma(\kappa_{1,l} - \kappa_{2,k})}, \end{aligned} \quad (19)$$

and can be further expressed via only the dominant term(s) based on the similar explanation as given for the CDF case earlier except with $\min(\xi, \alpha, \beta, 1, 1 + \epsilon)$ instead of $\min(\xi, \alpha, \beta)$, where ϵ is a very small error introduced so as not to violate the conditions given in the Appendix, required to utilize (26). Alternatively, a **high SNR** asymptotic analysis may also be done by utilizing the moments as [27, Eqs. (8) and (9)]

$$\bar{C} \underset{\mu_r \gg 1}{\approx} \log(\mu_r) + \zeta, \quad (20)$$

where

$$\zeta = \left. \frac{\partial}{\partial n} AF_\gamma^{(n)} \right|_{n=0}. \quad (21)$$

The expression in (20) can be simplified to

$$\begin{aligned} \bar{C} \underset{\mu_r \gg 1}{\approx} & \log(\mu_r) + \left. \frac{\partial}{\partial n} AF_\gamma^{(n)} \right|_{n=0} \\ & = \log(\mu_r) + \left. \frac{\partial}{\partial n} \left(\frac{\mathbb{E}[\gamma^n]}{\mathbb{E}[\gamma]^n} - 1 \right) \right|_{n=0} \\ & = \log(\mu_r) + \left. \left(\frac{1}{\mathbb{E}[\gamma]^n} \frac{\partial}{\partial n} \mathbb{E}[\gamma^n] + \mathbb{E}[\gamma^n] \frac{\partial}{\partial n} \frac{1}{\mathbb{E}[\gamma]^n} \right) \right|_{n=0} \\ & = \log(\mu_r) + \left. \left(\frac{1}{\mathbb{E}[\gamma]^n} \frac{\partial}{\partial n} \mathbb{E}[\gamma^n] - \frac{\mathbb{E}[\gamma^n] \log(\mathbb{E}[\gamma])}{\mathbb{E}[\gamma]^n} \right) \right|_{n=0} \\ & = \log(\mu_r) + \left. \left(\frac{1}{\mathbb{E}[\gamma]^n} \frac{\partial}{\partial n} \mathbb{E}[\gamma^n] - \frac{\mathbb{E}[\gamma^n] \log(\mu_r)}{\mathbb{E}[\gamma]^n} \right) \right|_{n=0} \\ & = \left. \frac{\partial}{\partial n} \mathbb{E}[\gamma^n] \right|_{n=0}. \end{aligned} \quad (22)$$

Hence, we need to evaluate the first derivative of the moments at $n = 0$ for high SNR asymptotic approximation to the ergodic capacity. The first derivative of the moments is given as

$$\frac{\partial}{\partial n} \mathbb{E}[\gamma^n] = \frac{\xi^2 \Gamma(rn + \alpha) \Gamma(rn + \beta)}{(\alpha\beta)^{rn} (rn + \xi^2) \Gamma(\alpha) \Gamma(\beta)} \left\{ r [\psi(rn + \alpha) + \psi(rn + \beta) - \log(\alpha\beta)] + \log(\mu_r) - \frac{r}{rn + \xi^2} \right\} \mu_r^n, \quad (23)$$

where $\psi(\cdot)$ is the digamma (psi) function [37, Eq. (6.3.1)], [24, Eq. (8.360.1)]. Evaluating (23) at $n = 0$, we get

$$\bar{C} \underset{\mu_r \gg 1}{\approx} \log(\mu_r) + r \left[\psi(\alpha) + \psi(\beta) - \log(\alpha\beta) - \frac{1}{\xi^2} \right]. \quad (24)$$

Hence, (24) gives the required expression for \bar{C} at high SNR in terms of simple elementary functions.

Furthermore, for **low SNR** asymptotic analysis, it can be easily shown that the ergodic capacity can be asymptotically approximated by the first moment. We can utilize (10) via placing $n = 1$ in it and hence the ergodic capacity of a single FSO link can be approximated at low SNR in closed-form in terms of simple elementary functions by

$$\bar{C} \underset{\mu_r \ll 1}{\approx} \mathbb{E}[\gamma^{n=1}] = \frac{\xi^2 \Gamma(r + \alpha) \Gamma(r + \beta)}{(\alpha\beta)^r (r + \xi^2) \Gamma(\alpha) \Gamma(\beta)} \mu_r. \quad (25)$$

V. NUMERICAL RESULTS AND DISCUSSION

As an illustration of the mathematical formalism presented above, simulation results for different performance metrics of a single FSO link transmission system is presented in this section. The FSO link is modeled as Gamma-Gamma fading channel with the effects of atmosphere for weak ($\alpha = 2.902$; $\beta = 2.51$), moderate ($\alpha = 2.296$; $\beta = 1.822$), and strong ($\alpha = 2.064$; $\beta = 1.342$) turbulence FSO channels [41, Table I].⁴

The OP is presented in Fig. 1 for both types of detection techniques (i.e. IM/DD and heterodyne) across the normalized average SNR with fixed effect of the pointing error ($\xi = 1$). We can observe from Fig. 1 that the simulation results provide a perfect match to the analytical results obtained in this work. It can be observed that heterodyne detection, being more complex method of detection technique as discussed earlier in the introduction section, performs much better than the IM/DD technique. Additionally, it can be observed that as the effect of atmospheric turbulence decreases, the performance improves. It can be seen that at high SNR, the asymptotic expression derived in (6) (i.e. utilizing all the terms in the summation) converges quite fast to the exact result proving this asymptotic approximation to be tight enough. Based on the effects of the fading parameters and the pointing error, the appropriate dominant term(s) can be selected as has been discussed earlier under the CDF sub-section. Hence, we can see that these respective dominant term(s) also converge

⁴It is important to note here that these values for the parameters were selected from the cited references subject to the standards to prove the validity of the obtained results and hence other specific values can be used to obtain the required results by design communication engineers before deployment.

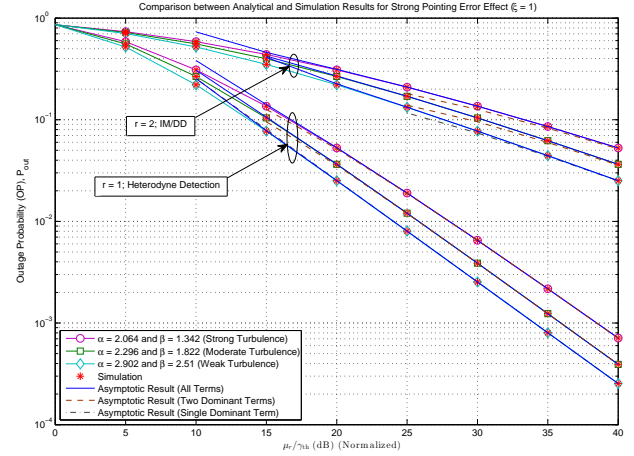


Fig. 1. OP showing the performance of both the detection techniques (heterodyne and IM/DD) under weak, moderate, and strong turbulent FSO channels.

though relatively slower, specially for the IM/DD technique. Similarly, Fig. 2 presents the OP for varying effects of pointing error ($\xi = 1$ and 6.7) under the IM/DD technique. We can

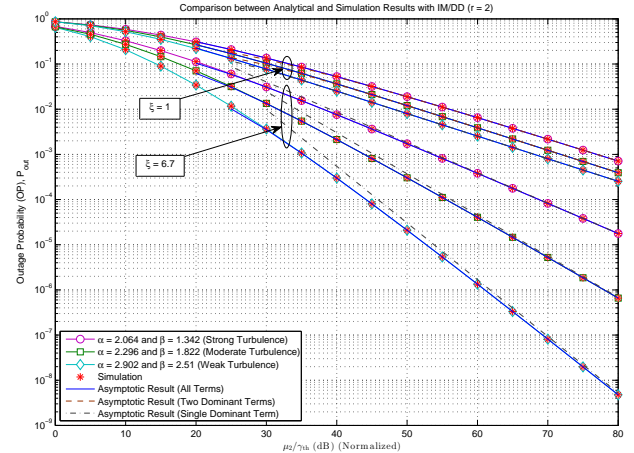


Fig. 2. OP showing the performance of IM/DD technique under weak, moderate, and strong turbulent FSO channels with varying effects of pointing error.

observe that for lower effect of the pointing error (i.e. higher value of ξ), the respective performance gets better manifolds. Other outcomes, specially for the asymptotic approximations, can be observed similar to Fig. 1 above.

The average BER performance of differential binary phase shift keying (DBPSK) binary modulation scheme is presented in Fig. 3 based on the values of p and q as presented in Table I where $p = 1$ and $q = 1$ represents DBPSK. The effect of pointing error is fixed at $\xi = 1$. We can observe from Fig. 3 that the simulation results provide a perfect match to the analytical results obtained in this work. It can also be observed that the heterodyne detection technique performs better than the IM/DD technique. Additionally, it can be observed that as the

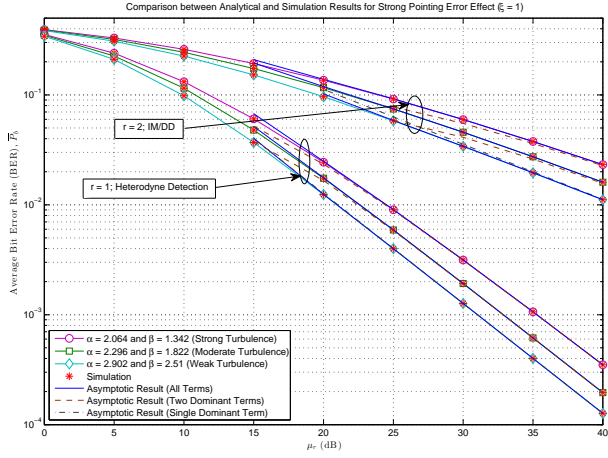


Fig. 3. Average BER of DBPSK binary modulation scheme showing the performance of both the detection techniques (heterodyne and IM/DD) under weak, moderate, and strong turbulent FSO channels.

effect of atmospheric turbulence decreases, the performance gets better. It can be seen that at high SNR, the asymptotic expression derived in (16) (i.e. utilizing all the terms in the summation) converges quite fast to the exact result proving its tightness. Based on the effects of the fading parameters and the pointing error, the appropriate dominant term(s) are selected and we can see that these respective dominant term(s) also converge though relatively slower, specially for the IM/DD technique. Similarly, Fig. 4 presents the average BER for varying effects of pointing error ($\xi = 1$ and 6.7) under the IM/DD technique. We can observe that for lower effect of

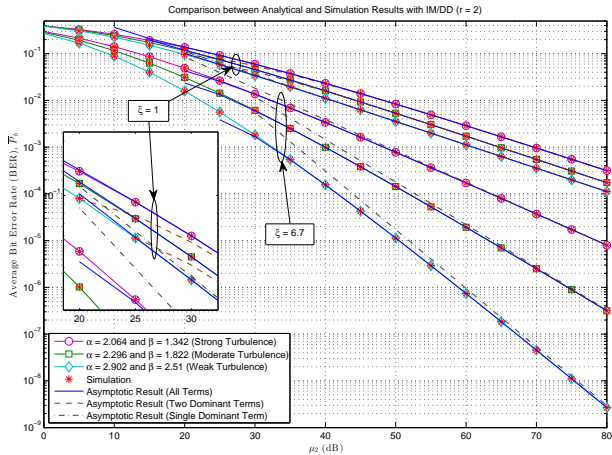


Fig. 4. Average BER of DBPSK binary modulation scheme showing the performance of IM/DD technique under weak, moderate, and strong turbulent FSO channels for varying effects of pointing error.

the pointing error ($\xi \rightarrow \infty$), the respective performance gets better manifolds. Other outcomes, specially for the asymptotic approximations, can be observed similar to Fig. 3 above.

In Fig. 5 and Fig. 6, the ergodic capacity of FSO channel in operation under IM/DD technique is demonstrated for varying

effects of pointing error, $\xi = 1.2$ and 6.7 . Expectedly,

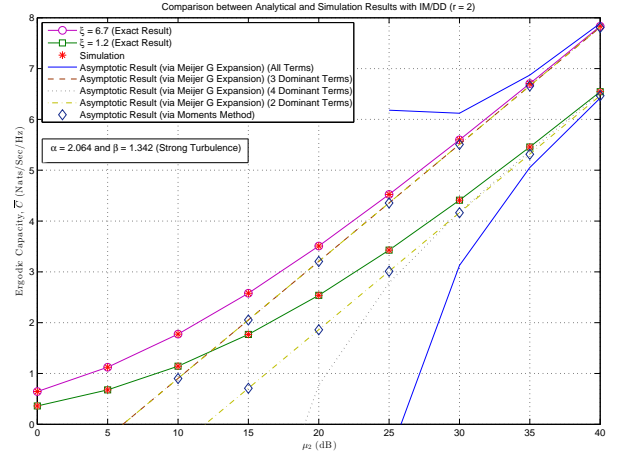


Fig. 5. Ergodic capacity results for the IM/DD technique under strong turbulence conditions for varying pointing errors along with the asymptotic results in high SNR regime.

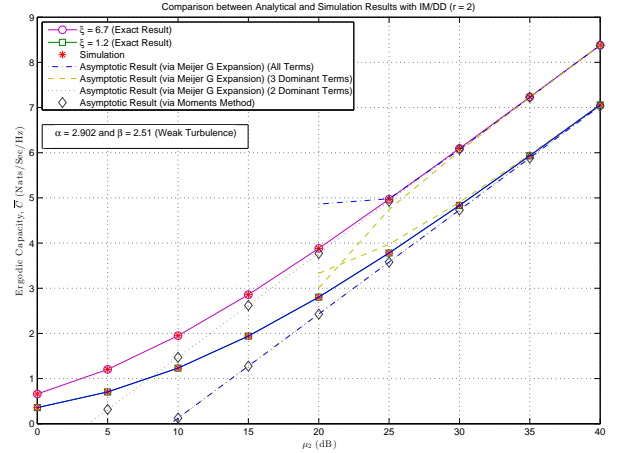


Fig. 6. Ergodic capacity results for the IM/DD technique under weak turbulence conditions for varying pointing errors along with the asymptotic results in high SNR regime.

as the atmospheric turbulence conditions get severe and/or as the pointing error gets severe, the ergodic capacity starts decreasing (i.e. the higher the values of α and β , and/or ξ , the higher will be the ergodic capacity). One of the most important outcomes of Fig. 5 and Fig. 6 are the asymptotic results for the ergodic capacity via two different methods. It can be seen that at high SNR, the asymptotic expression, via Meijer's G function expansion, derived in (19) (i.e. utilizing all the terms in the summation) converges rather slowly. Based on the effects of the fading parameters and the pointing error, the appropriate dominant term(s) are selected and we can see that these respective dominant term(s) also converge though relatively quite faster than the case where we employ all the terms. On the other hand, the asymptotic expression, via

utilizing moments, derived in (24) gives very tight asymptotic results in high SNR regime. Interestingly enough, it can be clearly seen that the two-dominant terms of (19) (derived via Meijer's G function expansion) signified by the two 1's present in the Meijer's G function of the exact ergodic capacity results in (18) and (24) (derived via moments) overlap. Finally, Fig. 7 presents tight asymptotic results for the ergodic capacity in low SNR regime derived in (25).

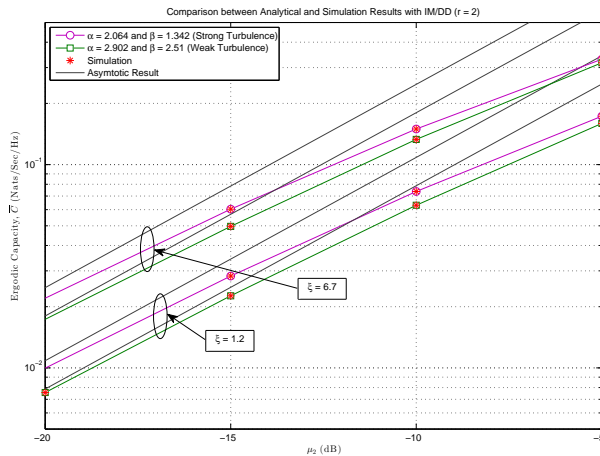


Fig. 7. Exact ergodic capacity results for the IM/DD technique under weak and strong turbulence conditions for varying pointing errors along with the asymptotic results in low SNR regime.

VI. CONCLUDING REMARKS

We presented unified expressions for the PDF, the CDF, the MGF, and the moments of the average SNR of an FSO link. Capitalizing on these expressions, we presented new unified formulas for various performance metrics including the OP, the higher-order AF, the error rate of a variety of modulation schemes, and the ergodic capacity in terms of Meijer's G function except for the higher-order AF that was in terms of simple elementary functions. Further, we derived and presented novel asymptotic expressions for the OP, the average BER, and the ergodic capacity in terms of basic elementary functions via utilizing Meijer's G function expansion given in the Appendix and via utilizing moments too for the ergodic capacity approximations. In addition, this work presented simulation examples to validate and illustrate the mathematical formulation developed in this work and to show the effect of the atmospheric turbulence conditions severity and the pointing errors severity on the system performance.

APPENDIX: MEIJER'S G FUNCTION EXPANSION

The Meijer's G function can be expressed, at a very low value of its argument, in terms of basic elementary functions via utilizing Meijer's G function expansion in [42, Theorem

1.4.2, Eq. (1.4.13)] and $\lim_{x \rightarrow 0^+} {}_cF_d[e; f; x] = 1$ [43] as

$$\lim_{z \rightarrow 0^+} G_{p,q}^{m,n} \left[z \left| \begin{matrix} a_1, \dots, a_n, \dots, a_p \\ b_1, \dots, b_m, \dots, a_q \end{matrix} \right. \right] = \sum_{k=1}^n z^{a_k-1} \times \frac{\prod_{l=1; l \neq k}^n \Gamma(a_k - a_l) \prod_{l=1}^m \Gamma(1 + b_l - a_k)}{\prod_{l=n+1}^p \Gamma(1 + a_l - a_k) \prod_{l=m+1}^q \Gamma(a_k - b_l)}, \quad (26)$$

where $a_k - a_l \neq 0, \pm 1, \pm 2, \dots; (k, l = 1, \dots, n; k \neq l)$ and $a_k - b_l \neq 1, 2, 3, \dots; (k = 1, \dots, n; l = 1, \dots, m)$.

REFERENCES

- [1] S. Haykin, "Cognitive radio: Brain-empowered wireless communications," *IEEE Journal on Selected Areas in Communications*, vol. 23, no. 2, pp. 201–220, Feb. 2005.
- [2] W. O. Popoola and Z. Ghassemloo, "BPSK subcarrier intensity modulated free-space optical communications in atmospheric turbulence," *IEEE/OSA Journal of Lightwave Technology*, vol. 27, no. 8, pp. 967–973, Apr. 2009.
- [3] L. C. Andrews, R. L. Phillips, and C. Y. Hopen, *Laser Beam Scintillation with Applications*. Bellingham, WA: SPIE, 2001.
- [4] K. P. Peppas and C. K. Datsikas, "Average symbol error probability of general-order rectangular quadrature amplitude modulation of optical wireless communication systems over atmospheric turbulence channels," *IEEE/OSA Journal of Optical Communications and Networking*, vol. 2, no. 2, pp. 102–110, Feb. 2010.
- [5] J. Park, E. Lee, and G. Yoon, "Average bit error rate of the Alamouti scheme in Gamma-Gamma fading channels," *IEEE Photonics Technology Letters*, vol. 23, no. 4, pp. 269–271, Feb. 2011.
- [6] M. Safari and M. Uysal, "Relay-assisted free-space optical communication," *IEEE Transactions on Wireless Communications*, vol. 7, no. 12, pp. 5441–5449, Dec. 2008.
- [7] S. M. Navidpour, M. Uysal, and M. Kavehrad, "BER performance of free-space optical transmission with spatial diversity," *IEEE Transactions on Wireless Communications*, vol. 6, no. 8, pp. 2813–2819, Aug. 2007.
- [8] I. S. Ansari, F. Yilmaz, and M.-S. Alouini, "Impact of pointing errors on the performance of mixed RF/FSO dual-hop transmission systems," *IEEE Wireless Communications Letters*, vol. 2, no. 3, pp. 351–354, Jun. 2013.
- [9] H. G. Sandalidis, T. A. Tsiftsis, G. K. Karagiannidis, and M. Uysal, "BER performance of FSO links over strong atmospheric turbulence channels with pointing errors," *IEEE Communications Letters*, vol. 12, no. 1, pp. 44–46, Jan. 2008.
- [10] H. G. Sandalidis, T. A. Tsiftsis, and G. K. Karagiannidis, "Optical wireless communications with heterodyne detection over turbulence channels with pointing errors," *IEEE/OSA Journal of Lightwave Technology*, vol. 27, no. 20, pp. 4440–4445, Oct. 2009.
- [11] W. Gappmair, "Further results on the capacity of free-space optical channels in turbulent atmosphere," *IET Communications*, vol. 5, no. 9, pp. 1262–1267, Jun. 2011.
- [12] T. A. Tsiftsis, "Performance of heterodyne wireless optical communication systems over Gamma-Gamma atmospheric turbulence channels," *Electronics Letter*, vol. 44, no. 5, pp. 372–373, Feb. 2008.
- [13] C. Liu, Y. Yao, Y. Sun, and X. Zhao, "Average capacity for heterodyne FSO communication systems over Gamma-Gamma turbulence channels with pointing errors," *Electronics Letters*, vol. 46, no. 12, pp. 851–853, Jun. 2010.
- [14] H. E. Nistazakis, T. A. Tsiftsis, and G. S. Tombras, "Performance analysis of free-space optical communication systems over atmospheric turbulence channels," *IET Communications*, vol. 3, no. 8, pp. 1402–1409, Aug. 2009.
- [15] M. Feng, J.-B. Wang, M. Sheng, L.-L. Cao, X.-X. Xie, and M. Chen, "Outage performance for parallel relay-assisted free-space optical communications in strong turbulence with pointing errors," in *Proceedings of International Conference on Wireless Communications and Signal Processing (WCSP' 11)*, Nanjing, China, Nov. 1990, pp. 1–5.
- [16] H. Li-Qiang, W. Qi, and S. Katsunori, "Outage probability of free space optical communication over atmosphere turbulence," in *Proceedings of WASE International Conference on Information Engineering (ICIE' 10)*, Beidaihe, Hebei, China, Aug. 2010, pp. 127–130.
- [17] Y. Ren, A. Dang, B. Luo, and H. Guo, "Capacities for long-distance free-space optical links under beam wander effects," *IEEE Photonics Technology Letters*, vol. 22, no. 14, pp. 1069–1071, Jul. 2010.

- [18] H. E. Nistazakis, E. A. Karagianni, A. D. Tsigopoulos, M. E. Fafalios, and G. S. Tombras, "Average capacity of optical wireless communication systems over atmospheric turbulence channels," *IEEE/OSA Journal of Lightwave Technology*, vol. 27, no. 8, pp. 974–979, Apr. 2009.
- [19] I. S. Ansari, F. Yilmaz, and M.-S. Alouini, "On the performance of mixed RF/FSO dual-hop transmission systems," in *Proceedings of the 77th IEEE Vehicular Technology Conference (VTC Spring' 2013)*, Dresden, Germany, Jun. 2013.
- [20] M. D. Springer, *The Algebra of Random Variables*. New York: Wiley, Apr. 1979.
- [21] O. M. Hasan, "Bit error rate and outage rate results for non-zero turbulence cells over Gamma-Gamma free-space optical wireless channel," *Journal of Optical Communications*, vol. 34, no. 4, pp. 1–7, 2013.
- [22] M. Niu, J. Cheng, and J. F. Holzman, "Error rate performance comparison of coherent and subcarrier intensity modulated optical wireless communications," *IEEE/OSA Journal of Optical Communications and Networking*, vol. 5, no. 10, pp. 554–564, Jun. 2013.
- [23] N. Wang and J. Cheng, "Moment-based estimation for the shape parameters of the Gamma-Gamma atmospheric turbulence model," *Optics Express*, vol. 18, no. 12, pp. 12 824–12 831, Jun. 2010.
- [24] I. S. Gradshteyn and I. M. Ryzhik, *Table of Integrals, Series and Products*. New York: Academic Press, 2000.
- [25] I. Wolfram Research, *Mathematica Edition: Version 8.0*. Champaign, Illinois: Wolfram Research, Inc., 2010.
- [26] C. K. Datsikas, K. P. Peppas, N. C. Sagias, and G. S. Tombras, "Serial free-space optical relaying communications over Gamma-Gamma atmospheric turbulence channels," *IEEE/OSA Journal of Optical Communications and Networking*, vol. 2, no. 8, pp. 576–586, Aug. 2010.
- [27] F. Yilmaz and M.-S. Alouini, "Novel asymptotic results on the high-order statistics of the channel capacity over generalized fading channels," in *Proceedings of IEEE 13th International Workshop on Signal Processing Advances in Wireless Communications (SPAWC' 2012)*, Cesme, Turkey, Jun. 2012, pp. 389–393.
- [28] U. Charash, "Reception through Nakagami fading multipath channels with random delays," *IEEE Transactions on Communications*, vol. 27, no. 4, pp. 657–670, Apr. 1979.
- [29] I. S. Ansari, S. Al-Ahmadi, F. Yilmaz, M.-S. Alouini, and H. Yanikomeroğlu, "A new formula for the BER of binary modulations with dual-branch selection over generalized- K composite fading channels," *IEEE Transactions on Communications*, vol. 59, no. 10, pp. 2654–2658, Oct. 2011.
- [30] N. C. Sagias, D. A. Zogas, and G. K. Kariaginidis, "Selection diversity receivers over nonidentical Weibull fading channels," *IEEE Transactions on Vehicular Technology*, vol. 54, no. 6, pp. 2146–2151, Nov. 2005.
- [31] A. H. Wojnar, "Unknown bounds on performance in Nakagami channels," *IEEE Transactions on Communications*, vol. 34, no. 1, pp. 22–24, Jan. 1986.
- [32] I. S. Ansari, F. Yilmaz, and M.-S. Alouini, "On the sum of Gamma random variates with application to the performance of maximal ratio combining over Nakagami- m fading channels," in *Proceedings of IEEE 13th International Workshop on Signal Processing Advances in Wireless Communications (SPAWC' 2012)*, Cesme, Turkey, Jun. 2012, pp. 394–398.
- [33] X. Song, M. Niu, and J. Cheng, "Error rate of subcarrier intensity modulations for wireless optical communications," *IEEE Communications Letters*, vol. 16, no. 4, pp. 540–543, Apr. 2012.
- [34] M. Niu, X. Song, J. Cheng, and J. F. Holzman, "Performance analysis of coherent wireless optical communications with atmospheric turbulence," *Optics Express*, vol. 20, no. 6, pp. 6515–6520, Mar. 2012.
- [35] Z. Wang and G. B. Giannakis, "A simple and general parameterization quantifying performance in fading channels," *IEEE Transactions on Communications*, vol. 51, no. 8, pp. 1389–1398, Aug. 2003.
- [36] M.-S. Alouini and A. J. Goldsmith, "A unified approach for calculating error rates of linearly modulated signals over generalized fading channels," *IEEE Transactions on Communications*, vol. 47, no. 9, pp. 1324–1334, Sep. 1999.
- [37] M. Abramowitz and I. A. Stegun, *Handbook of Mathematical Functions*, 10th ed. New York: Dover, Dec. 1972.
- [38] F. Yilmaz, O. Kucur, and M.-S. Alouini, "A novel framework on exact average symbol error probabilities of multihop transmission over amplify-and-forward relay fading channels," in *Proceedings of 7th International Symposium on Wireless Communication Systems (ISWCS' 2010)*, York, U.K., Nov. 2010, pp. 546–550.
- [39] V. S. Adamchik and O. I. Marichev, "The algorithm for calculating integrals of hypergeometric type functions and its realization in reduce system," in *Proceedings of International Symposium on Symbolic and Algebraic Computation (ISSAC' 90)*, New York, USA, 1990, pp. 212–224.
- [40] C. Liu, Y. Yao, Y. Sun, and X. Zhao, "Analysis of average capacity for free space optical links with pointing errors over Gamma-Gamma turbulence channels," *Chinese Optics Letters*, vol. 8, no. 6, pp. 537–540, Jun. 2010.
- [41] X. Tang, Z. Ghassemlooy, S. Rajbhandari, W. O. Popoola, and C. G. Lee, "Coherent polarization shift keying modulated free space optical links over a Gamma-Gamma turbulence channel," *American Journal of Engineering and Applied Sciences*, vol. 4, no. 4, pp. 520–530, 2011.
- [42] A. M. Mathai and R. K. Saxena, *Generalized Hypergeometric Functions with Applications in Statistics and Physical Sciences*, Lecture Notes in Mathematics, vol. 348. Springer-Verlag, 1973.
- [43] M. D. Renzo, A. Guidotti, and G. E. Corazza, "Average rate of downlink heterogeneous cellular networks over generalized fading channels: a stochastic geometry approach," *IEEE Transactions on Communications*, vol. 61, no. 7, pp. 3050–3071, Jul. 2013.